TU Delft

Delft University of Technology

# SIW Based Antenna Array with Power Equalization in Elevation Plane for 5G Base Stations

Puskely, Jan; Aslan, Yanki; Roederer, Antoine; Yarovoy, Alexander

**DOI**
10.1049/cp.2018.0424

**Publication date**
2018

**Document Version**
Final published version

**Published in**
Proceedings - 12th European Conference on Antennas and Propagation, EUCAP 2018

**Citation (APA)**
Puskely, J., Aslan, Y., Roederer, A., & Yarovoy, A. (2018). SIW Based Antenna Array with Power Equalization in Elevation Plane for 5G Base Stations. In *Proceedings - 12th European Conference on Antennas and Propagation, EUCAP 2018* (pp. 1-5). Institution of Engineering and Technology. https://doi.org/10.1049/cp.2018.0424

**Important note**
To cite this publication, please use the final published version (if applicable).
Please check the document version above.

**Copyright**
Other than for strictly personal use, it is not permitted to download, forward or distribute the text or part of it, without the consent of the author(s) and/or copyright holder(s), unless the work is under an open content license such as Creative Commons.

**Takedown policy**
Please contact us and provide details if you believe this document breaches copyrights.
We will remove access to the work immediately and investigate your claim.

*This work is downloaded from Delft University of Technology.*
*For technical reasons the number of authors shown on this cover page is limited to a maximum of 10.*

***Green Open Access added to TU Delft Institutional Repository***

***'You share, we take care!' – Taverne project***

***https://www.openaccess.nl/en/you-share-we-take-care***

Otherwise as indicated in the copyright section: the publisher is the copyright holder of this work and the author uses the Dutch legislation to make this work public.

# SIW Based Antenna Array with Power Equalization in Elevation Plane for 5G Base Stations

Jan Puskely, Yanki Aslan, Antoine Roederer, Alexander Yarovoy
MS3, Department of Microelectronics, Delft University of Technology, Mekelweg 4, 2628CD Delft, Netherlands
J.Puskely-1@tudelft.nl, Y.Aslan@tudelft.nl, A.G.Roederer@tudelft.nl, A.Yarovoy@tudelft.nl

***Abstract*— In this paper, we present a 5G base station phased array antenna concept based on the power flux equalization in the elevation plane. We designed an aperture-coupled microstrip patch sub-array fed by a substrate integrated waveguide to produce a cosecant radiation pattern in the elevation plane. The antenna is designed to be operational at frequencies around 28.5GHz, targeting a candidate 5G mm-wave frequency band. The dimensions of the cosecant antenna sub-array support wide-angle scanning of the final phased array antenna in the horizontal plane. The antenna exhibits good impedance and radiation properties in the scanning range +/- 45deg.**

***Index Terms*—5G base station, phased array antenna, microstrip patch antenna, substrate integrated waveguide, cosecant radiation pattern.**

## I. INTRODUCTION

The fifth generation (5G) technologies for cellular systems are gaining worldwide attention. Compared with 4G systems, the 5G system is shifted to higher frequencies where it is easier to satisfy the demands of the 5G network targeting higher data rates and improved quality of service [1-2]. To achieve the expected data rates, 5G base station antenna systems will have to guarantee a high level of flexibility and high performances [2] (e.g., real-time adaptive beamforming, multi beam generation).

In mm-waves, the current research interest for 5G applications is on two frequency band candidates, 28GHz and 38GHz [3]. However, the development of high performance and low-cost antenna array systems at such frequencies bring new challenges to be addressed for the success of 5G cellular wireless technologies [2, 4-6].

In this paper, we propose a 5G base station concept of phased array antenna based on linear sub-arrays with cosecant beam pattern in the vertical plane, synthesized to get uniform flux over a coverage area [7]. Several linear array designs with cosecant-squared power pattern exist in the literature [8-10]. However, unlike those designs, the proposed sub-array is based on aperture-coupled microstrip patch antennas (AC-MPA) [11] fed by a substrate integrated waveguide (SIW).

SIW is easily manufactured at low cost for mass production by making densely arrayed via-holes and metal-plating the surfaces. The measured transmission loss of the SIW at $K_a$-band is small, around 0.05 dB/cm. Exploiting a SIW structure for MPA feeding combines the benefits of both structures. It results in a compact antenna structure retaining the advantageous properties of MPAs and having a radiation characteristic without the spurious radiation that is usually produced by a conventional feeding line.

The antenna is designed to be operational at frequencies around 28.5GHz, targeting the candidate 5G frequency band. The sub-array has optimal electrical dimensions to support wide-angle scanning in the horizontal plane. Hereafter we will show that the antenna exhibits good impedance and radiation properties in the scanning range +/- 45deg .

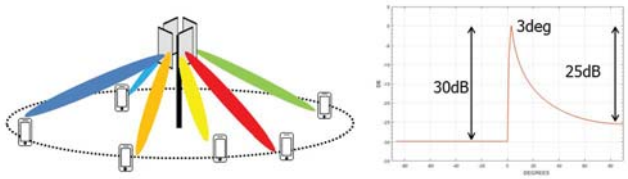


Fig. 1. 5G base station concept based on flux equalization in elevation cut; Defined mask of a cosecant radiation pattern in the elevation plane.

## II. DESIGN OF A SUB-ARRAY WITH COSECANT RADIATION PATTERN

The cosecant shaped-beam series-fed aperture-coupled microstrip patch sub-array has been designed as a basic element for the active phased array antenna. The whole antenna system is designed with the aid of CST MS.

### *A. AC-MPA element fed by SIW*

The structure of the proposed AC- MPA fed by SIW with its overall dimensions is depicted in Fig. 2.

The basic antenna element consists of two dielectric layers, a SIW layer and a patch layer. The rectangular microstrip patch of width $W_p$ and length $L_p$ is placed on the top surface of the patch layer with relative permittivity 2.2 and thickness $t_{s1}$. The microstrip patch is aperture coupled through the longitudinal slot ($L_{sl}$, $W_{sl}$) integrated to the SIW layer with relative permittivity 2.2 and thickness $t_{s2}$. The slot is centered on the maximum of the standing waveguide wave at a distance $d_3$ from the waveguide end wall and has an offset $d_1$ from the centre line of the SIW. The patch is placed symmetrically to the centre of the slot. The via is used as tuning element in the final cosecant subarray design.

To simplify the antenna modelling, the SIW is replaced by an equivalent RWG of width $W_{eqSIW}$ and length $L_{eqSIW}$ with solid walls [12]. This approach significantly reduces the

simulation runtime. The port on the left side of the SIW excites the fundamental TE10 mode. The other end of the SIW is shorted. The dimensions of the element are listed in Table I.

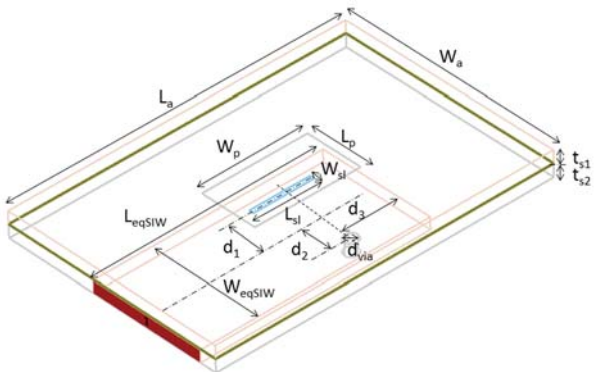


Fig. 2. The geometry of the SIW-fed AC-MPA.

TABLE I. DIMENSIONS OF THE ANTENNA ELEMENT IN FIG. 2

| Parameters | Value [mm] | Parameters | Value [mm] |
|---|---|---|---|
| $L_a$ | 14.700 | $W_{eqSIW}$ | 5.050 |
| $W_a$ | 9.800 | $d_1$ | 1.660 |
| $L_p$ | 2.500 | $d_2$ | 1.600 |
| $W_p$ | 4.600 | $d_3$ | 2.600 |
| $L_{sl}$ | 2.600 | $d_{via}$ | 0.600 |
| $W_{sl}$ | 0.200 | $t_{s1}$ | 0.508 |
| $L_{eqSIW}$ | 9.900 | $t_{s2}$ | 0.508 |

The computed input reflection coefficient of the SIW antenna is presented in Fig. 3. The characteristic impedance was matched to 50Ω in the simulations. The antenna operational band is centered at 28.45GHz with bandwidth of about 2.9GHz (BW ~ 10%). The resonant frequency of the SIW element can be shifted by changing the length of the patch $L_p$. The antenna radiation patterns at the center of the operational band are presented in Fig. 4. It can be observed that the antenna has symmetrical radiation pattern. A gain above 7.5dB and low levels of cross-polarization in main planes are obtained in the whole operational band.

### B. *Design of an AC-MPA Sub-Array with Cosecant Radiation Pattern*

As a trade-off between gain and maximum sub-array dimension, a linear sub-array of twelve radiators is chosen. The sub-array is shown in Fig. 5. At the operating frequency, the coupling slots are centered at the peaks of the guided wave ($d_P$ = 4.98mm; 0.53λ at 28.5GHz). The centre of the last slot is placed a quarter guided wavelength from the end wall. The total dimensions of the array are $L_{ar}$ = 71mm and $W_{ar}$ = 9.8mm.

An approach based on Elliott's design procedure for the slotted waveguide arrays [13] is used for the design of an AC-MPA array fed by a SIW. The self-admittance $Y$ of an isolated antenna element is extracted using the two port structure similar to that shown in Fig. 2. The self-admittance is normalised to the characteristic conductance $G_0$ of the RWG is obtained by optimizing the slot length $L_{SL}$, the patch

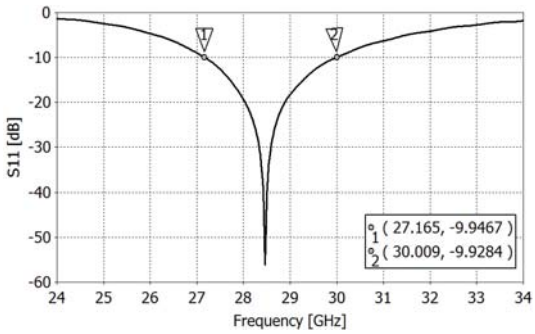


Fig. 3. Computed input reflection coefficients of the SIW-fed MPA.

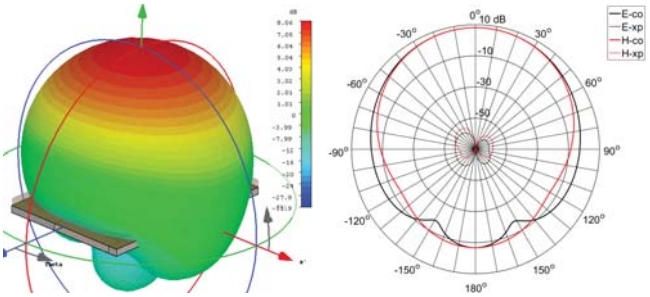


Fig. 4. Computed radiation patterns at 28.5 GHz.


Fig. 5. Cosecant linear sub-array of twelve AC-MPA elements fed by a SIW.

length $L_p$ and via position $d_v$ and it is given by [13]

$$Y/G_0 = G/G_0 + j\,B/G_0 = -2s_{11}/(1+s_{11}). \quad (1)$$

The linear sub-array of AC-MPAs is impedance matched through the desired frequency band while the sum of normalized conductances $G/G_0$ of each element in the sub-array is equal to one at the operating frequency. Similarly, the sum of normalized susceptances $B/G_0$ should be zero.

To reach the required cosecant radiation pattern in the H-plane, amplitude and phase distribution were synthesized in an initial step (initial values are in Table I). The mask shown in Fig. 1 has been taken as a reference in the synthesis process. In the next step, to simplify the design of the array, the phase distribution was taken as uniform and the amplitude distribution was further optimized. The final excitation coefficients are listed in Table II. The cosecant radiation pattern related to the given excitation coefficients is depicted in Fig. 8. On the basis of the amplitude distribution, the required values of $G/G_0$ of each radiators were achieved.

Six AC-MPAs having the required values of $G/G_0$ were realized by optimizing the dimensions mentioned in the previous paragraph. In optimization process, mutual coupling between the antenna elements was not taken into account for simplicity. In Fig. 6, it can be seen that the resultant normalized components of $Y/G_0$ of the isolated antenna

elements agree with the required ones. The final AC-MPAs dimensions differ in the slot length $L_{SL}$, the patch length $L_p$ and position of the via $d_v$ compensating the capacitive character of the radiator. The other parameters, such as $d_{SL}$, $W_p$ and $W_{SL}$, are common for all. The parameters are listed in Table III. To realize a phase shift of 54deg between the first and second element, the length of the SIW was increased corresponding to the given guided wave, i.e. $d_{FI} = 1.51$mm.

TABLE II. EXCIATATION COEFFICIENTS FOR THE COSECANT BEAM PATTERN

| Num. elem. | Initial excit. coeff. | | Optim. excit. coeff. | | G/G$_0$ |
|---|---|---|---|---|---|
| | Ampl | Phase [deg] | Ampl | Phase [deg] | |
| 1 | 0.481 | 206 | 0.481 | 206 | 0.232 |
| 2 | 0.407 | 152 | 0.407 | 152 | 0.166 |
| 3 | 0.315 | 150 | 0.317 | 152 | 0.100 |
| 4 | 0.328 | 132 | 0.317 | 152 | 0.100 |
| 5 | 0.266 | 134 | 0.266 | 152 | 0.071 |
| 6 | 0.269 | 124 | 0.266 | 152 | 0.071 |
| 7 | 0.228 | 126 | 0.224 | 152 | 0.050 |
| 8 | 0.225 | 118 | 0.224 | 152 | 0.050 |
| 9 | 0.204 | 120 | 0.199 | 152 | 0.040 |
| 10 | 0.197 | 114 | 0.199 | 152 | 0.040 |
| 11 | 0.189 | 117 | 0.199 | 152 | 0.040 |
| 12 | 0.183 | 112 | 0.199 | 152 | 0.040 |

TABLE III. DESIGN PARAMETERS OF SUB-ARRAY ELEMENTS IN MM

| n.e. $x$ | $L_{SL}$ | $W_{SL}$ | $d_{SL}$ | $L_P$ | $W_P$ | $d_v$ |
|---|---|---|---|---|---|---|
| 1 | 2.34 | 0.20 | 1.00 | 2.48 | 4.20 | 2.00 |
| 2 | 2.64 | 0.20 | 1.00 | 2.28 | 4.20 | 2.00 |
| 3-4 | 2.71 | 0.20 | 1.00 | 2.05 | 4.20 | 2.00 |
| 5-6 | 2.64 | 0.20 | 1.00 | 2.04 | 4.20 | 2.07 |
| 7-8 | 2.67 | 0.20 | 1.00 | 1.84 | 4.20 | 2.09 |
| 9-12 | 2.64 | 0.20 | 1.00 | 1.79 | 4.20 | 2.13 |

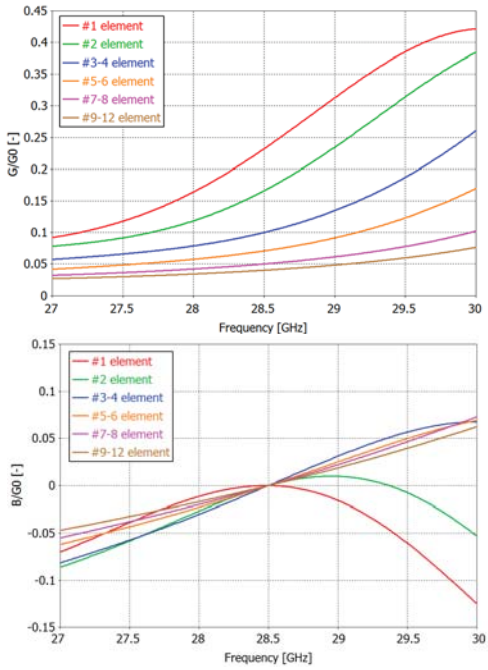


Fig. 6. Simulated normalised self-admittances of isolated radiating elements; top) $G/G_0$; bottom) $B/G_0$.

The simulated results of the cosecant linear SIW-fed AC-MPA sub-array with the parameters listed in Table III are depicted in Fig. 7 and Fig. 8. The simulated reflection coefficient indicates an impedance bandwidth of about 10% for $s_{11} < -10$dB (28-31GHz). The radiation pattern in the H-plane has a maximum gain of 15.7 dB and shows good agreement with patterns based on isolated radiating elements. The radiation pattern in the E-plane shows a small asymmetry caused by unequal excitations of AC-MPAs. The asymmetry is about 1dB.

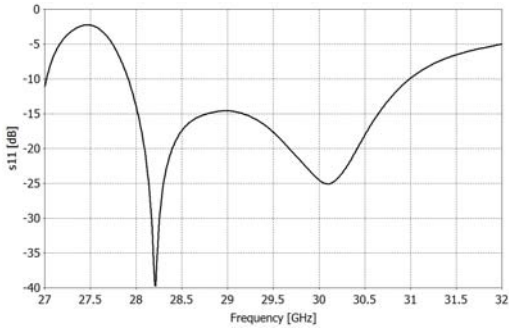


Fig. 7. Reflection coefficient of the AC-MPA sub-array.

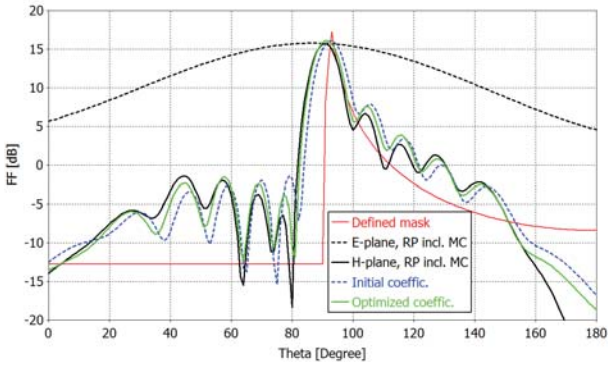


Fig. 8. Radiation patterns of the AC-MPA sub-array at 28.5GHz .

### C. *Infinite Antenna Array Performances*

To analyze the scanning performance of the SIW AC-MPA sub-array in a phased array antenna, the width of the sub-array has to be changed to size around 0.5λ at 28.5GHz. The antenna array with a width of $W_{ar} = 5.3$mm is depicted in Fig. 9.

How this change affects the impedance and radiation properties of the sub-array is also shown in Fig. 9 (better impedance matching, less gain). This width provides the possibility to achieve scanning over more than +/- 60deg without grating lobes in the azimuthal plane.

The active reflection coefficient as a function of the scan angle in the azimuthal plane is shown in Fig. 10. The variation is more constrained in the range +/-30deg in the whole band 28-31GHz. However, the scanning performance is still maintained for scan angles up to +/-45deg, but with a smaller bandwidth of 28-29.5GHz, which is still acceptable for 5G applications. The scanning performance of the array in the E-plane (azimuthal plane) is presented in the next section.

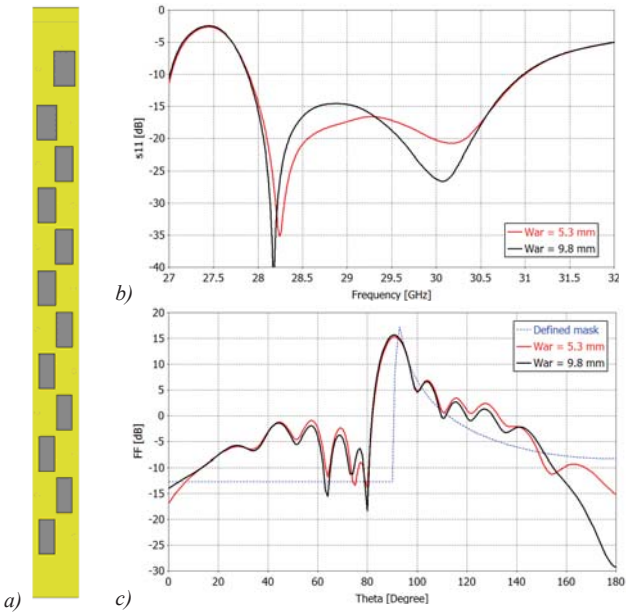


Fig. 9. a) Structure of the linear AC-MPA sub-array in an infinite array; with related b) impedance properties and c) radiation properties in the H-plane.

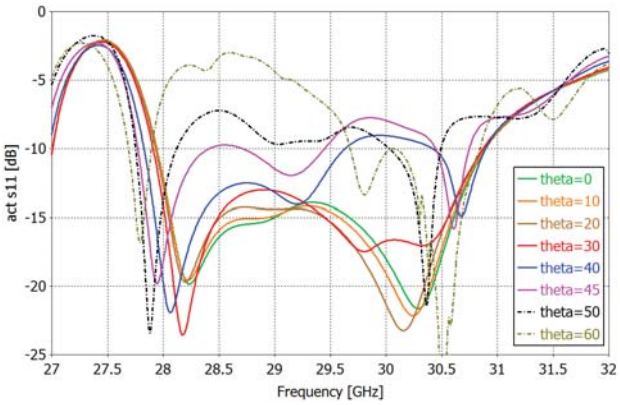


Fig. 10. Active reflection coefficients of the infinite array in the azimuthal plane.

## III. Dense Phased Array Antenna Concept

In order to analyse the scanning capabilities and to verify the active reflection coefficients of the sub-array from the previous section, the finite phased array antenna of 16 cosecant sub-arrays was designed (Fig. 11). The total dimensions of the phased array are 70x85mm$^2$. A uniform amplitude distribution is considered for the beam scanning analysis.

The reflection coefficients for different scan angles are presented in Fig. 12. Results were calculated for all cosecant sub-arrays in the phased array. The computed results correspond to those of the infinite array of Fig. 10. In the scanning range +/- 45deg, the operational bandwidth defined as $s_{11} < -8$dB is about 10% (28-31GHz). The same operational bandwidth could be obtained also for the highest analysed scanning angle but with a worse impedance matching $s_{11} < -6$dB.

Perfect impedance matching is obtained only in a limited frequency range between 28.0-28.3GHz for scanning angles within +/-45deg. The scan radiation patterns for this frequency band are depicted in Fig. 13. A grating-lobe-free beam scanning range of up to +/-60deg is achieved. The maximum level of side lobes is below -13 dB in the whole scanning range. The reduction in side lobe level can be achieved by dedicated amplitude tapering.

The mentioned asymmetry of the cosecant sub-array in the E-plane plays a role in the final radiation pattern of the phased array. It is obvious that the realized gain in the E-plane is smaller in scanning range of -20deg to -45deg and it is about 1dB less at -45deg compared with the realized gain at +45deg. Nevertheless, the radiation patterns confirm our assumption in terms of scan loss in the range +/-45deg. The scan loss is 1.4dB at 45deg and 2.3dB at -45deg.

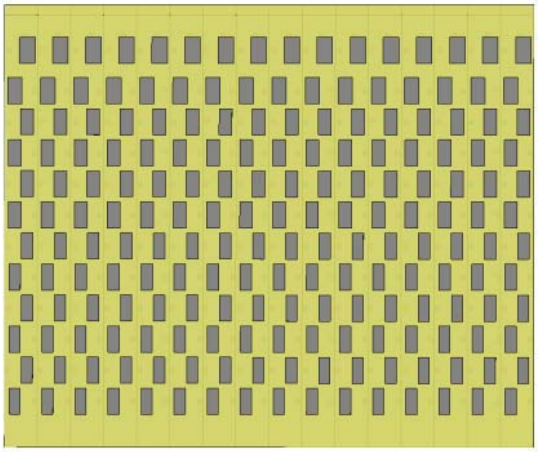

Fig. 11. Structure of the array of 16 sub-array of twelve elements.

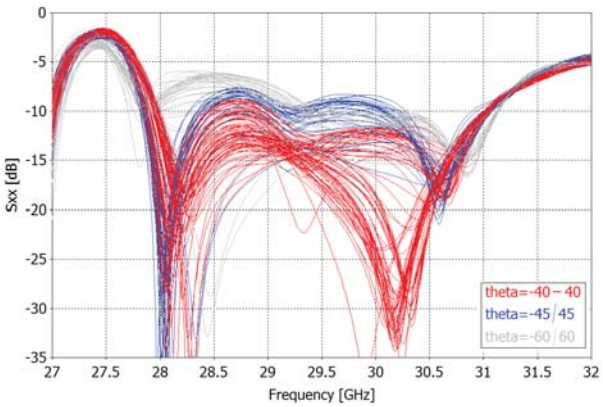


Fig. 12. Simulated active reflection coefficients of the cosecant sub-arrays for different scanning angles.

## IV. Conclusions

A sub-array of SIW-fed aperture-coupled patches producing a cosecant pattern in elevation was designed in order to get uniform flux over a coverage area. An array of such sub-arrays has been evaluated and produces wide angle scanning in azimuth. The phased array antenna is aimed to 5G base stations for operation around 28GHz.

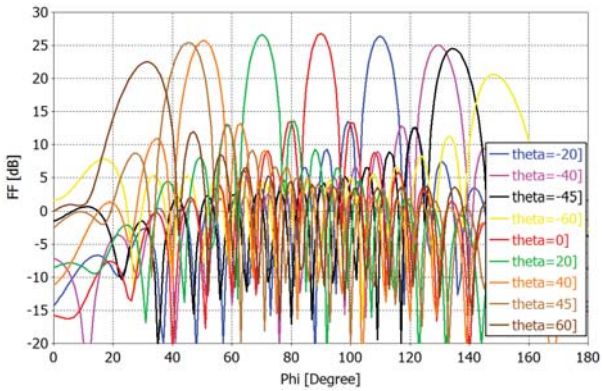


Fig. 13. Scanning performance of the phased array at 28.2GHz (Realized gain).

## ACKNOWLEDGMENT

This research was conducted as part of the STW-NXP Partnership Program on Advanced 5G Solutions within the project titled "Antenna Topologies and Front-end Configurations for Multiple Beam Generation". For further information: www.nwo.nl.

## REFERENCES

[1] C. X. Wang, F. Haider, X. Gao, X.-H. You, Y. Yang, D. Yuan, H. M. Aggoune, H. Haas, S. Fletcher, E. Hepsaydir, "Cellular architecture and key technologies for 5G wireless communication networks, " *IEEE Commun. Mag*., vol. 52, no. 2, pp. 122-130, Feb. 2014.

[2] D. Muirhead, M. A. Imran and K. Arshad, "A survey of the challenges, opportunities and use of multiple antennas in current and future 5G small cell base stations," *IEEE Access*, vol. 4, pp. 2952-2964, 2016.

[3] A. I. Sulyman, A. T. Nassar, M. K. Samimi, G. R. Maccartney, T. S. Rappaport, and A. Alsanie, "Radio propagation path loss models for 5G cellular networks in the 28 GHZ and 38 GHZ millimeter-wave bands, " *IEEE Commun. Mag*., vol. 52, no. 9, pp. 78-86, 2014.

[4] G. Oliveri *et al*., "Co-Design of Unconventional Array Architectures and Antenna Elements for 5G Base Stations," in *IEEE Transactions on Antennas and Propagation*, vol. PP, no. 99, pp. 1-1.

[5] W. Hong, K. H. Baek, Y. Lee, Y. Kim and S. T. Ko, "Study and prototyping of practically large-scale mmWave antenna systems for 5G cellular devices," in *IEEE Communications Magazine*, vol. 52, no. 9, pp. 63-69, September 2014.

[6] M. H. Dahri, M. H. Jamaluddin, M. I. Abbasi and M. R. Kamarudin, "A Review of Wideband Reflectarray Antennas for 5G Communication Systems," in *IEEE Access*, vol. 5, pp. 17803-17815, 2017.

[7] Elliot, R. S., and G. J. Stern, "A new technique for shaped beam synthesis of equispaced arrays," *IEEE Trans. Antennas Propag*., 32(10), 1129–1133, 1984.

[8] J. Hirokawa, C. Yamazaki and M. Ando, "Postwall waveguide slot array with cosecant radiation pattern and null filling for base station antennas in local multidistributed systems," in *Radio Science*, vol. 37, no. 2, pp. 1-7, April 2002.

[9] M. Koubeissi, L. Freytag, C. Decroze and T. Monediere, "Design of a Cosecant-Squared Pattern Antenna Fed by a New Butler Matrix Topology for Base Station at 42 GHz," in *IEEE Antennas and Wireless Propagation Letters*, vol. 7, pp. 354-357, 2008.

[10] S. Chen *et al*., "Azimuth scanning, Ka-band phased array antenna," *IEEE Antennas and Propagation Society International Symposium. 2001 Digest. Held in conjunction with: USNC/URSI National Radio Science Meeting (Cat. No.01CH37229)*, Boston, MA, USA, 2001, pp. 808-811 vol.3.

[11] T. Mikulasek, J. Lacik, J. Puskely and Z. Raida, "Design of aperture-coupled microstrip patch antenna array fed by SIW for 60 GHz band," in *IET Microwaves, Antennas & Propagation*, vol. 10, no. 3, pp. 288-292, 2 19 2016.

[12] Yan, L., Hong,W., Wu, K., Cui, T.J.: "Investigations on the propagation characteristics of the substrate integrated waveguide based on the method of lines," *IEE Proc. Microw. Antennas Propag*., 2005, 152, (1), pp. 35–42

[13] Elliott, R.S.: "Antenna theory and design " (John Wiley & Sons, Inc., Hoboken (NJ), 2003, Revised edn., Chapter VIII)